Synoptic controls upon δ^{18}O in southern Tasmanian precipitation

Vaughan J. I. Barras[1] and Ian Simmonds[2]

Received 27 August 2007; revised 22 October 2007; accepted 10 December 2007; published 19 January 2008.

[1] An event-based record of ^{18}O in precipitation at Margate in Tasmania, Australia, was analysed using 3d Lagrangian trajectories and composites of ERA40 850hPa geopotential height for the years 1994–2002. Trajectory analysis found that moisture entrainment occurs during the 48 hour period prior to arrival for all precipitating air masses at Margate. The rate of entrainment was greatest for events of high rainfall/high depletion, contributing up to 19% of vapour in the air mass in summer and up to 47% in winter. The majority of air masses were found to be advected from the Southern Ocean, however, for high rainfall/high depletion events during summer 30% of air masses were found to approach from the Tasman Sea (east of 155E longitude). Mean isotope ratios were less depleted by 1.4‰ for these events indicating mixing with less depleted air. High rainfall/high depletion events were also associated with negative geopotential anomalies east of Tasmania.
Citation: Barras, V. J. I., and I. Simmonds (2008), Synoptic controls upon δ^{18}O in southern Tasmanian precipitation, *Geophys. Res. Lett.*, *35*, L02707, doi:10.1029/2007GL031835.

1. Introduction

[2] The variability of the stable water isotope ratio ^{18}O/^{16}O in natural archives of precipitation is a valuable interpretative tool in hydrological studies. In recent years, regional paleoclimate studies have successfully used ^{18}O/^{16}O ratios (hereafter ^{18}O) sourced from speleothems [*Xia et al.*, 2001; *McDermott*, 2004] and event-based precipitation [*Burnett et al.*, 2004; *Treble et al.*, 2005] to assist in reconstructions of regional atmospheric circulation. The recent development of high precision sampling techniques now provides the capability of obtaining speleothem records of isotopic variability with weekly resolution in some cases [*Frappier et al.*, 2007]. Although there is still much to learn about the processes involved in interpreting speleothem isotope ratios on these timescales, it is possible to use existing records of ^{18}O in event-based precipitation records to determine potential synoptic controls upon isotopic content and yield information about the circulation and structure of the atmosphere.

[3] It is well established that atmospheric circulation plays a major role in the modification of ^{18}O throughout the hydrological cycle [*Dansgaard*, 1964]. The effects of storm track location, seasonal deposition and local synoptic circulation upon the isotopic content of precipitation are important considerations in the use of records of ^{18}O as an indicator of paleoclimatic conditions [*Lawrence et al.*, 1982; *Noone and Simmonds*, 1998]. In the midlatitudes, the isotopic ratio of an individual precipitation event depends upon the prevailing synoptic circulation and local convective and evaporative processes [*Lawrence et al.*, 1982; *Gedzelman and Lawrence*, 1982]. Subsequently, records of isotopic variability in precipitation collected on synoptic timescales in this region may act as natural archives of synoptic circulation and storm intensity. Previous analyses have often combined surface pressure fields and the calculation of air mass trajectories, and have associated the isotopic content of precipitation with particular circulation features and recent moisture history [*Gedzelman and Lawrence*, 1982; *Friedman et al.*, 2002; *Burnett et al.*, 2004]. The studies of *Schlosser et al.* [2004] and *Helsen et al.* [2006] combined 3d Lagrangian back trajectories from reanalyses with results from isotope models of varying cloud complexity in reconstructions of snow pit accumulation at sites in Antarctica. Using this approach, the authors were able to not only characterize the evaporation environment from fluctuations in parcel temperature and specific humidity but also simulate the subsequent isotopic fractionation during air mass approach.

[4] Records of ^{18}O in precipitation have been collected and analysed at two locations in Tasmania, Australia: Margate on the southeast coast and Cape Grim in the far northwest used for baseline air sampling from the Southern Ocean (Figure 1a). Tasmania is a midlatitude environment of considerable interest in that precipitating air masses have little interaction with land or high topography throughout their history from source region to site of precipitation. Corresponding deuterium measurements for these records were unable to be made. A recent analysis of 5 years of these records by *Treble et al.* [2005] found an inverse relationship between ^{18}O and rainfall amount at the Margate site and only a weak relationship with surface temperature. Using composite maps of surface pressure, events of high rainfall and high depletion were associated with more proximal centres of low pressure. To further investigate the synoptic control upon ^{18}O in Tasmanian precipitation, an analysis of updated records of δ^{18}O in precipitation collected at both at Cape Grim and Margate was performed for the period 1994–2002 using 3d Lagrangian back trajectories and composite maps of surface pressure and geopotential height, however in the interests of brevity only selected results for the Margate site are presented here. From this, the effects of air mass source region, moisture entrainment during approach and the influence of local atmospheric circulation upon ^{18}O are investigated.

2. Data and Analytical Method

[5] Samples of precipitation were collected at 8am local time following a rain day at the Margate observing site.

[1]Bureau of Meteorology Research Centre, Melbourne, Victoria, Australia.
[2]School of Earth Sciences, University of Melbourne, Melbourne, Victoria, Australia.

0094-8276/08/2007GL031835

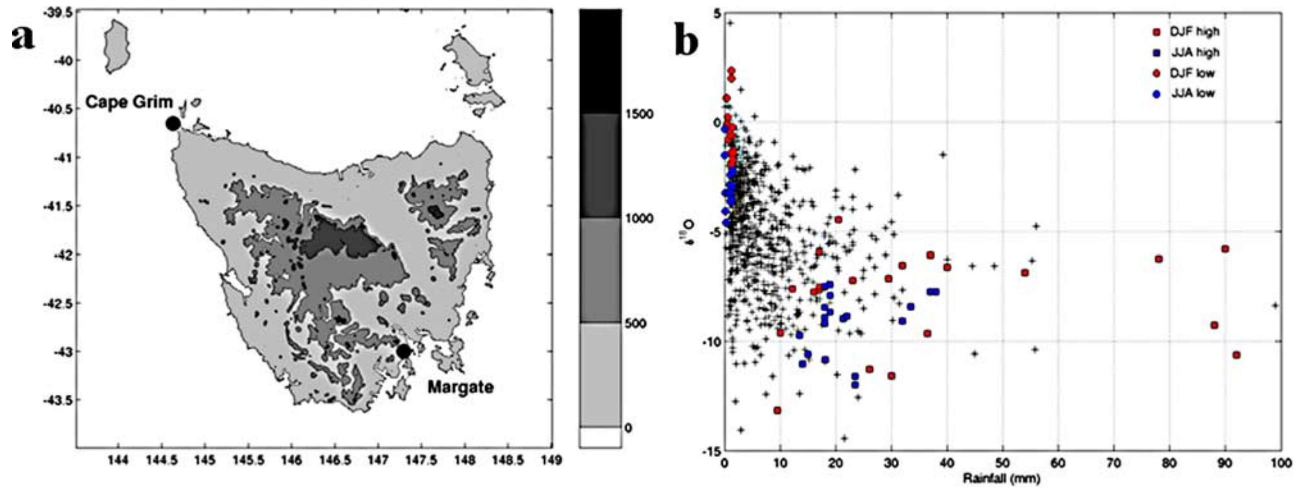

Figure 1. (a) Topographical map of Tasmania with locations of Cape Grim and Margate observing sites. Contour interval is 500m. (b) Plot of Margate δ^{18}O versus rainfall. Events selected for analysis highlighted.

These were collected by W. Budd and periodically analysed for ^{18}O using a VG Micromass SIRA Series II mass spectrometer by V. Morgan at the University of Tasmania. Results were reported in 'δ' notation measured against the Vienna Standard Mean Ocean Water (VSMOW) reference standard such that $\delta = (R/R_{std} - 1) \times 1000$ where R is the ratio ^{18}O/^{16}O. In this study, rain samples with large negative values of δ^{18}O are referred to as highly depleted. Where multiple samples were analysed, the measurement accuracy was found to be better than ±0.1‰. As a test of the possible effects of time spent in storage, samples were measured at two separate dates 10 weeks apart. Differences were found to be no greater than the instrument measurement accuracy over this period. Storage periods were regularly no greater than 6–12 months, although on the rare occasion where storage periods were greater than this, a weak evaporative enrichment of samples is possible.

[6] The resulting data is negatively skewed about a mean of −4.8‰ with a standard deviation of 2.7‰ (Figure 1b) and have been found to be negatively correlated with rainfall amount [*Treble et al.*, 2005]. After weighting by mass, the data was then filtered to remove the background seasonal variability. The upper and lowermost deciles for the summer (DJF) and winter (JJA) periods (each comprising 20 events) were then classified as 'extreme' with mean isotope ratios of −6.8‰, −0.6‰ and −8.4‰, −3.4‰ respectively. These extreme categories are referred to in this paper as high rainfall/high depletion and low rainfall/low depletion events.

[7] Backward trajectories were calculated for each event using a 3d Lagrangian trajectory scheme developed by *Noone and Simmonds* [1999]. ERA40 precipitation [*Uppala et al.*, 2005] was found to have a close correspondence with the occurrence of rainfall events in the Margate observations, although tending to underestimate rainfall amount in some of the high depletion cases. Wind fields (u, v and w), temperature (T) and specific humidity (q) were read into the trajectory scheme at 6-hourly intervals, and the trajectory path was then calculated backwards in time using cubic interpolation for spatial data and linear interpolation between timesteps to determine the values of T and q along the advection path. Trajectories were calculated for several vertical levels at 1 hour intervals out to 96 hours prior to arrival to illustrate the immediate moisture history of the air masses associated with each event, however no concurrent isotopic calculations were available. Uncertainties in the calculated air mass location by the 3d trajectory scheme are generally less than 1000km out to 144 hours [*Noone and Simmonds*, 1999], therefore the 96 hour trajectories here may be regarded as sufficiently accurate for the purposes of this study. Composite seasonal anomalies of mean sea level pressure and geopotential height were also calculated for each of the extreme categories using data from the ERA40 reanalysis. The significance of the differences of the composite mean anomalies from the seasonal climatological mean were tested using a student's t-test.

3. Results

3.1. Backward Trajectories in 3-D

[8] Trajectories arriving at 950hPa, 850hPa and 500hPa were calculated for events of high rainfall/high depletion and low rainfall/low depletion. Particular attention was drawn to the identification of major sources of remote isotopic modification from large scale condensation, such as the effect of rainout from extended advection over land or forced ascent over high topography [*Friedman et al.*, 2002]. Isotopic content may also vary on the synoptic scale due to condensation from uplift by poleward isentropic moisture transport or from the admixture of air masses along the trajectory.

[9] Results for trajectories arriving at 850hPa are presented here as an illustration of the approach path of precipitating air masses arriving at a characteristic cloud base level. A significance test of the centroids of the source regions for each category found no significant difference between the trajectories associated with events of high rainfall/high depletion (red) and low rainfall/low depletion cases (black) for either DJF or JJA (Figures 2a and 2b) reflecting the dominance of the westerly airstream across the Southern Ocean. In most cases, precipitating air masses arriving at 850hPa are advected eastward over the Southern Ocean with little exposure to land. Only a 5% increase was

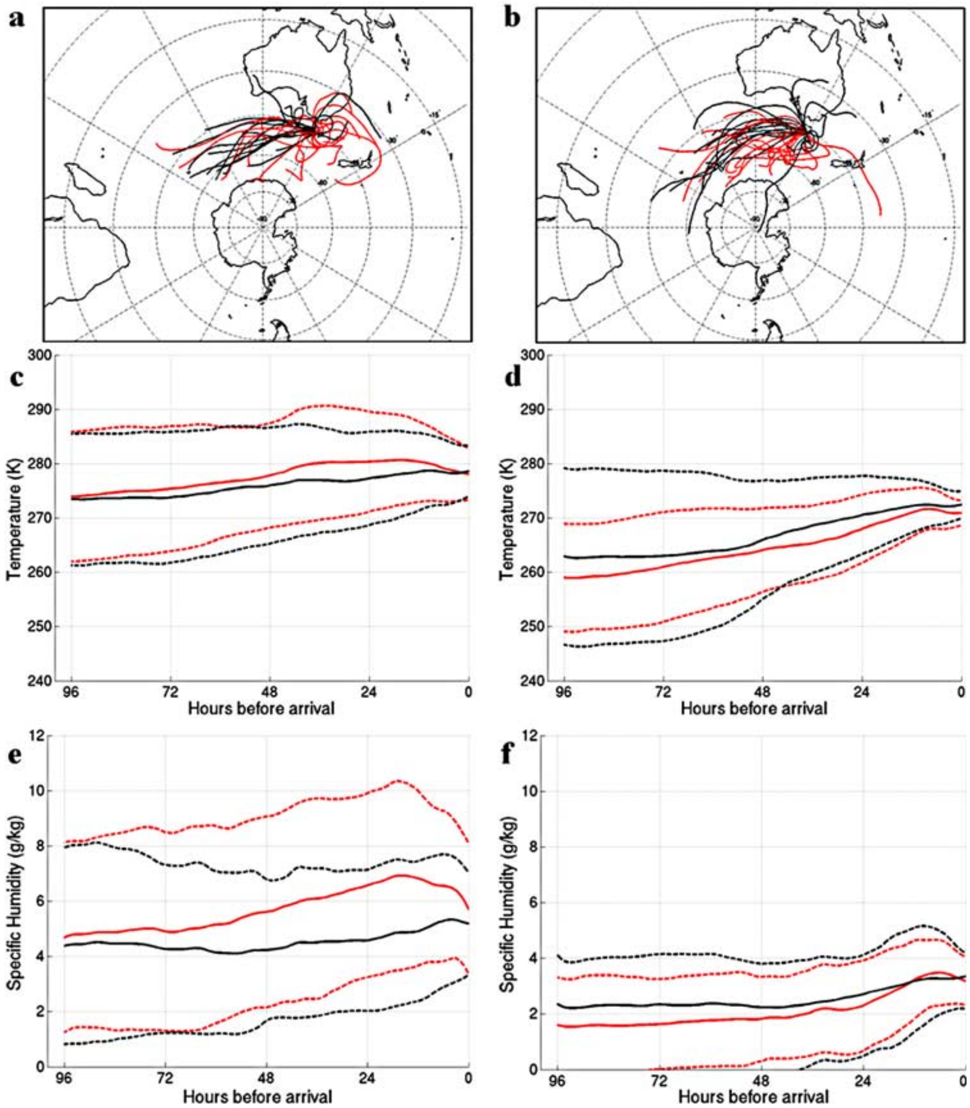

Figure 2. ERA40 96 hour 3-D trajectories arriving at 850hPa for high rainfall/high depletion (red) and low rainfall/low depletion cases (black) at Margate (a) DJF advection paths, (b) JJA advection paths, (c) DJF temperatures, (d) JJA temperatures, (e) DJF specific humidities, and (f) JJA specific humidities. Dotted lines indicate ± one standard deviation from mean trajectories.

found in the number of trajectories for DJF events of high rainfall/high depletion approaching from within 1 degree of longitude 6 hours prior to arrival (implying meridional approach) compared to the other categories. This agrees with *Treble et al.* [2005], however no significant difference was found in isotope content. Alternatively, we found that 30% of events in this category were advected from the Tasman Sea (origin east of 155E). Mean isotope ratios measured for these events were less depleted by 1.4‰ when compared to the remaining events within the category.

[10] Figures 2c, 2d, 2e and 2f show the fluctuations of temperature and specific humidity derived by the trajectory scheme that provide a good indication of the evaporation environment of each air mass during approach to Tasmania. Large or rapid changes in temperature or specific humidity may indicate condensation or the entrainment of moisture. For clarity, only the mean conditions for the Margate trajectories arriving at 850hPa have been plotted here, although there was a large range of values between individual trajectories.

[11] There are many similarities between the high and low rainfall/depletion categories, both in magnitude and variability (Figures 2c and 2d). For events in both DJF and JJA, a gradual warming of the air masses is observed during the period of approach which is, in part, associated with a gradual descent of the trajectories (not shown). The degree of warming can be seen to be greater for the JJA cases, however the differences in temperature between the two extreme categories for each season are always within ±4K. A similar comparison of mean specific humidity fluctuation does show a difference between the extreme categories, but only for DJF events (Figure 2e). Air masses associated with low rainfall/low depletion during this period experience a very small increase in specific humidity commencing 48 hours prior to arrival, whereas for events of high rainfall/high depletion the rate of increase is greater. This indicates

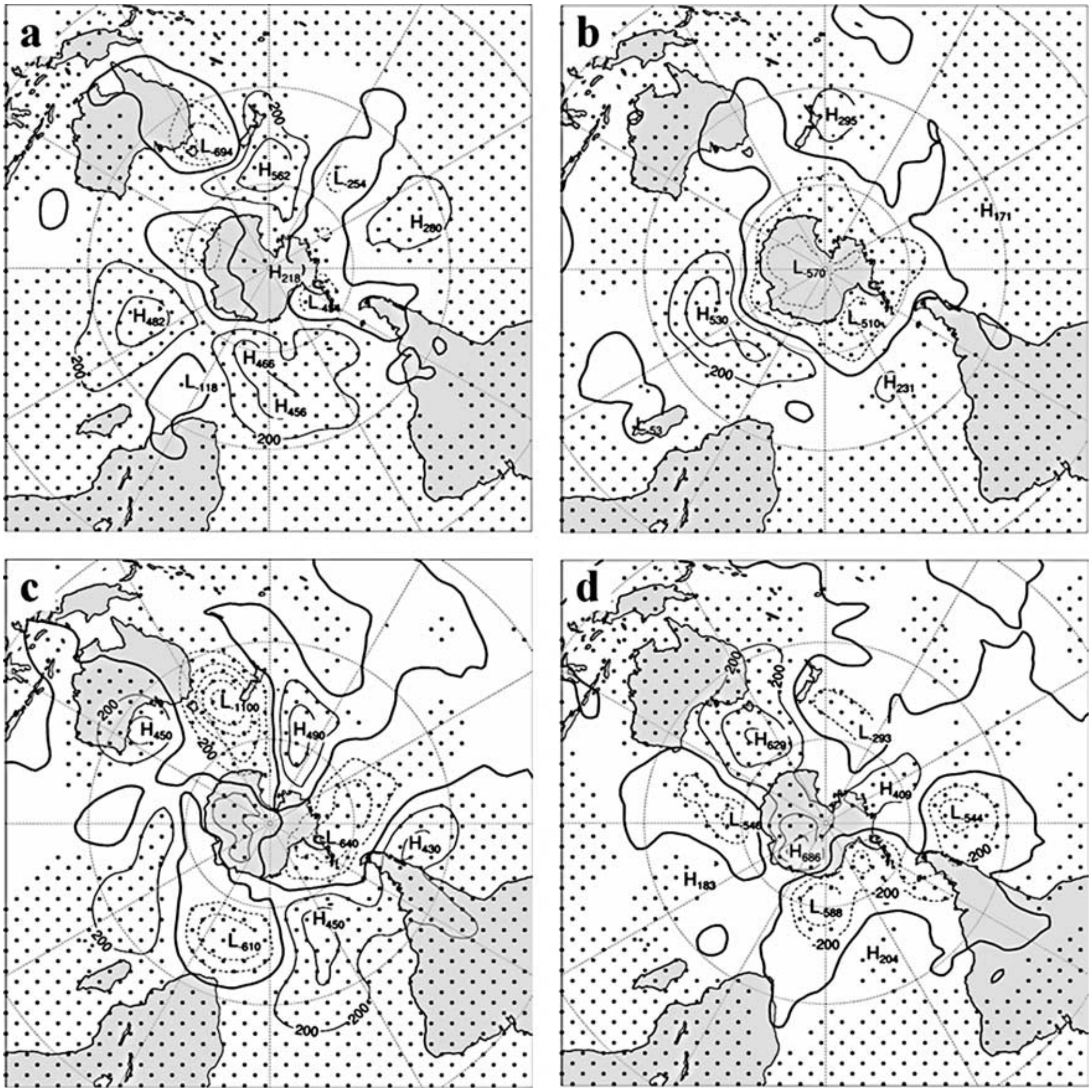

Figure 3. ERA40 composite daily 850hPa geopotential height seasonal anomalies for rainfall events at Margate (a) DJF events of high rainfall/high depletion, (b) DJF events of low rainfall/low depletion, (c) JJA events of high rainfall/high depletion, and (d) JJA events of low rainfall/low depletion. Stippling indicates anomalies significantly different from zero at the 95% confidence level.

an entrainment of moisture sourced from local evaporation or drawn from different latitudes. Few large decreases in specific humidity denoting possible rainout of heavy isotopes are seen prior to the onset of precipitation by which time entrained moisture for the high rainfall/high depletion events constitutes 19% of the total. Similarly, entrained moisture makes up nearly 47% of the high rainfall/high depletion events during JJA (Figure 2f), although the air masses are colder and drier at this time.

3.2. Synoptic Conditions

[12] Small differences between the trajectory profiles for each rainfall/depletion category indicate an influence of the synoptic scale circulation upon the evaporation environment. This confirms the findings from a previous analysis of the Margate isotope record by *Treble et al.* [2005] that emphasised the importance of the proximity of low pressure systems upon rainfall amount and local ^{18}O variability for the periods of winter-spring and summer-autumn.

[13] For the synoptic analysis presented here the focus was expanded to illustrate the circulation structure of the entire Southern Hemisphere associated with these events. Although this study uses an updated version of the isotope record used by *Treble et al.* [2005] and the seasonal periods chosen for this study differ slightly, similar synoptic patterns were observed with a well developed trough off the eastern coast of Tasmania associated with events of high rainfall/high depletion. Furthermore, the climatological anomaly patterns were found to be barotropic in nature, appearing throughout the low troposphere to the 500hPa level in analyses of geopotential height. The seasonal anomalies of geopotential height at the 850hPa level for rain events during DJF and JJA are presented in Figure 3 as an indication of the prevailing circulation structure. Regions

where anomalies are significantly different from zero above the 95% confidence level are stippled.

[14] Composite maps of geopotential height for the extreme categories for DJF shows a relatively strong negative geopotential anomaly off the east coast of Tasmania associated with events of high rainfall/high depletion (Figure 3a). Elsewhere, weak troughs are evident over the Pacific, South America, South Africa and the eastern Indian Ocean although only the last two appear significant. The positive anomaly poleward of New Zealand signifies a blocking of the circulation which may indicate a separation of cyclonic systems from the mean westerly flow during these highly depleted DJF events. The hemispheric 850hPa geopotential anomaly pattern differs substantially for low rainfall/low depletion events during DJF (Figure 3b). In the midlatitudes of the Australian region, no significant anomaly is found indicating that rainfall is associated with relatively mobile frontal systems embedded in a mean westerly flow.

[15] The anomaly patterns are similar but greater in magnitude for the JJA cases. Events of high rainfall/high depletion (Figure 3c) are associated with stronger seasonal anomalies. Although unlikely to be depicting a common stationary planetary wave pattern, the anomalies again indicate local trough development affecting the amounts and isotopic content of precipitation. The cases of low rainfall/low depletion during JJA (Figure 3d) show a similar synoptic circulation pattern although the sign of the anomalies has changed. There is a greater influence of anticyclonic ridging over southern Australia, drawing a more west to northwesterly airflow over Tasmania in association with weakening frontal systems. Air masses approaching Margate from this direction would be more influenced by the topography of the island than air approaching from other directions affecting rainfall distribution and isotope content due to continental exposure, enhanced rainout and droplet evaporative effects.

4. Discussion

[16] Analyses of air mass trajectories and circulation structure confirm a synoptic control upon ^{18}O in Tasmanian precipitation and the influence of moisture history upon air masses as they approach Tasmania. These findings are consistent with those of *Treble et al.* [2005] in that isotopic variability in local rainfall shows an association with rainfall amount and the proximity of low pressure systems. Furthermore, by observational analysis and reconstruction of 3d backward trajectories this study has demonstrated the importance of eastward trajectory origin and seasonal extent of moisture entrainment contributing to the enrichment of ^{18}O in precipitation in southern Tasmania.

[17] The trajectory analyses reveal that the majority of air masses approach from the Southern Ocean in the prevailing westerly airstream. However, changes in circulation bring about changes in rainfall amount that is the primary influence upon isotopic content in Tasmanian precipitation. In addition, it has been shown that circulation changes also alter the trajectory origins and moisture histories of air masses, further modifying the isotopic content of the resulting precipitation. Events of high rainfall/high depletion entrain the most moisture in the 48 hours prior to arrival, particularly during DJF. Observations from Margate have shown that entrainment of isotopically enriched moisture from local evaporation or from lower latitudes may explain unusually low depletion values measured during this time.

[18] Composite anomalies of 850hPa geopotential height show a well developed trough to the east of the island in the Tasman Sea is common to events of high rainfall/high depletion, in agreement with the findings of *Treble et al.* [2005]. This anomaly pattern is barotropic in structure and is reflected throughout the low troposphere to the 500hPa level. The mean synoptic anomaly patterns in Figure 3 are best viewed as an assembly of samples of the local transient flow rather than reflecting a common stationary planetary wave pattern. Conversely, the weak anomaly pattern for events of low rainfall/low depletion during DJF indicates predominantly zonal winds across the midlatitudes, with rain falling from mobile frontal systems. During JJA, fronts approaching Tasmania are substantially weakened under the influence of ridging over the Australian region.

[19] It has been demonstrated that isotope ratios in southern Tasmanian precipitation are modified by the local and large scale circulation in addition to precipitation amount and temperature which is important in understanding natural climate archives such as speleothems. In this regard, future studies would benefit from high resolution observations of precipitation and near surface water vapour in conjunction with modeling of contributing fractionation effects. We show here that the state of the local atmospheric circulation is an important control upon isotopic ratios of southern Tasmanian precipitation, therefore isotope archives resolved over similar timescales may be valuable as indicators of past circulation changes in the region.

[20] **Acknowledgments.** This study was supported by funding from the Australian Research Council, a Commonwealth Postgraduate Studentship from CSIRO Marine and Atmospheric Research, a research scholarship from the University of Melbourne, and a grant from the David Hay Memorial Fund. Thanks to David Etheridge, Bill Budd, Vin Morgan, and Laurie Porter for the provision of the isotope data and for valuable comments on the interpretation of the records.

References

Burnett, A. W., H. T. Mullins, and W. T. Patterson (2004), Relationship between atmospheric circulation and winter precipitation $\delta^{18}O$ in central New York State, *Geophys. Res. Lett.*, *31*, L22209, doi:10.1029/2004GL021089.

Dansgaard, W. (1964), Stable isotopes in precipitation, *Tellus*, *16*, 436–468.

Frappier, A. B., D. Sahagian, S. J. Carpenter, L. A. Gonzalez, and B. R. Frappier (2007), Stalagmite stable isotope record of recent tropical cyclone events, *Geology*, *35*, 111–114, doi:10.1130/G23145A.1.

Friedman, I., J. M. Harris, G. I. Smith, and C. A. Johnson (2002), Stable isotope compositions of waters in the Great Basin, United States: 1. Airmass trajectories, *J. Geophys. Res.*, *107*(D19), 4400, doi:10.1029/2001JD000565.

Gedzelman, S. D., and J. R. Lawrence (1982), The isotopic composition of cyclonic precipitation, *J. Appl. Meteorol.*, *21*, 1385–1404.

Helsen, M. M., R. S.W. van de Wal, M. R. van den Broeke, V. Masson-Delmotte, H. A.J. Meijer, M. P. Scheele, and M. Werner (2006), Modeling the isotopic composition of Antarctic snow using backward trajectories: Simulation of snow pit records, *J. Geophys. Res.*, *111*, D15109, doi:10.1029/2005JD006524.

Lawrence, J. R., S. D. Gedzelman, J. W.C. White, D. Smiley, and P. Lazov (1982), Storm trajectories in eastern US D/H isotopic composition of precipitation, *Nature*, *296*, 638–640.

McDermott, F. (2004), Palaeo-climate reconstruction from stable isotope variations in speleothems: A review, *Quat. Sci. Rev.*, *23*, 901–918.

Noone, D., and I. Simmonds (1998), Implications for the interpretation of ice-core isotope data from analysis of modelled Antarctic precipitation, *Ann. Glaciol.*, *27*, 398–402.
Noone, D., and I. Simmonds (1999), A three-dimensional spherical trajectory algorithm, in *Research Activities in Atmospheric and Oceanic Modelling*, edited by H. Ritchie, Rep. 28, World Meteorol. Organ., 3.26–3.27.
Schlosser, E., C. Reijmer, H. Oerter, and W. Graf (2004), The influence of precipitation origin on the $\delta^{18}O$-T relationship at Neumayer station, Ekströmisen, Antarctica, *Ann. Glaciol.*, *39*, 41–48.
Treble, P., W. F. Budd, P. K. Hope, and P. K. Rustomji (2005), Synoptic-scale climate patterns associated with rainfall $\delta^{18}O$ in southern Australia, *J. Hydrol.*, *302*, 270–282.
Uppala, S. M., et al. (2005), The ERA-40 re-analysis, *Q. J. R. Meteorol. Soc.*, *131*, 2961–3012.
Xia, Q., J. X. Zhao, and K. D. Collerson (2001), Early-mid Holocene climatic variations in Tasmania, Australia: Multi-proxy records in a stalagmite from Lynds cave, *Earth Planet. Sci. Lett.*, *194*, 177–187.

V. Barras, Bureau of Meteorology Research Centre, Melbourne, Victoria 3001, Australia. (v.barras@bom.gov.au)
I. Simmonds, School of Earth Sciences, University of Melbourne, Melbourne, Victoria 3010, Australia. (simmonds@unimelb.edu.au)